Journal of Applied Mechanics and Technical Physics, Vol. 46, No. 1, pp. 42–48, 2005

FORMATION OF SECONDARY DROPS DURING IMPACT INTERACTION OF A DROP WITH A LIQUID SURFACE

V. A. Arkhipov and V. F. Trofimov

UDC 532.529

This paper reports results from experimental studies of the formation of secondary drops during impact interaction of a drop with a liquid surface. The experimental data are compared with analytical estimates of the parameters of the cavern formed and the Rayleigh column.

Key words: *liquid surface, drop, secondary drops.*

The interaction of a falling drop with a liquid surface is a classical problem of hydrodynamics which has attracted the attention of researchers for many years [1–9]. Reviews on the problem in question are given in [5, 8]. The literature deals primarily with experimental studies of the qualitative picture of the interaction process [1–7]. A numerical solution of the problem of cavern collapse using the ideal fluid model is presented in [8, 9].

The physics of impact interaction of a drop with a liquid surface is of interest for the solution of a number of applied problems, such as the estimation of the depth of the crater produced by the cumulative effect of micrometeorite impact on the spacecraft body [6, 10], the determination of the parameters of underwater acoustic noise due to raindrop fall on a marine surface [7, 9], etc. In particular, an important ecological problem is predicting the propagation topology and dynamics of drops of toxic agents which are formed during precipitation on the surface of catch basins located on the territory of chemical plants, near nuclear facilities, etc. [11]. To solve this problem, it is necessary to know the quantitative mass–transfer characteristics and the parameters of the secondary drops produced by impact of precipitating drops on the liquid surface.

The present paper gives experimental results and analytical estimates for the quantitative characteristics of mass transfer during formation of secondary drops of various sizes produced by the impact interaction of a drop with a liquid surface.

Experimental Setup and Technique. The study was performed on a setup consisting of a generator of monodisperse drops, a system for visualizing the interaction of falling drops with a liquid surface, and a system for measuring the parameters of the falling drops before impact [12]. A diagram of the experimental setup is shown in Fig. 1. The liquid from the overhead tank 1 was supplied to a capillary 2 through a flow microregulator 3, which controlled the rate of drop formation. The overhead tank, flow regulator, and capillary were fixed on a support which adjusted the height of drop fall in the range $h = 0.07$–2.5 m. The drop formed at the polished end of the capillary fell in a tank 4 with dimensions $0.1 \times 0.1 \times 0.07$ m made of optical plane–parallel plates glued together. The optical transparency of the tank walls allowed the visualization and recording of the interaction of the falling drops with the surface and volume of the liquid in the tank 4. The interaction was recorded by an NV-DA1EG digital video camera or a Zenit–TTL mirror camera 5 provided with an electrical trigger 6. The electrical trigger was actuated by the signal of an amplifier 7. The signal actuating the electrical trigger was generated when the falling drop crossed the upper laser beam 8 directed to a photodetector 9. The signal then passed through a delay unit 10, which synchronized the drop–liquid interaction with the moment of opening of the camera shutter. By varying the shutter-opening delay in the range 0.1–1000 msec, we could record the interaction process at various time. Transmission recording was performed using a flash lamp or a continuous-operation photographic bulb as a

Institute of Applied Mathematics and Mechanics, Tomsk State University, Tomsk 634050; leva@niipmm.tsu.ru. Translated from Prikladnaya Mekhanika i Tekhnicheskaya Fizika, Vol. 46, No. 1, pp. 55–62, January–February, 2005. Original article submitted October 1, 2003; revision submitted May 12, 2004.

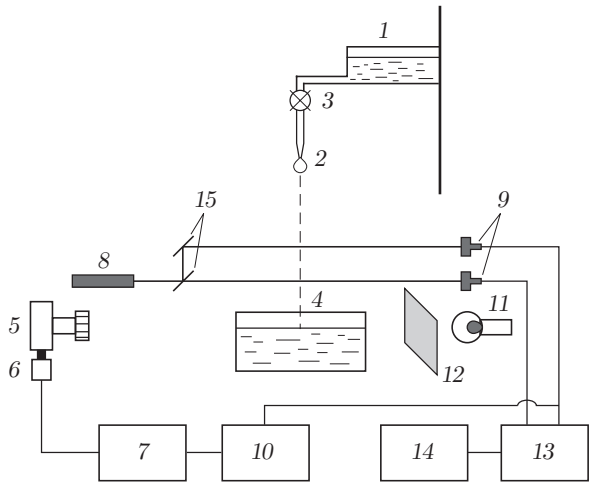

Fig. 1. Experimental setup for studying drop impact on a liquid surface.

light source 11. The light from the source 1 was dispersed onto an opaque screen 12, which allowed variation in the illumination intensity. During adjustment of the optical system of the setup, the axis of the video camera or photographic camera was in the plane of the liquid surface, which made it possible to record the processes occurring both below and above the liquid surface.

To determine the number and parameters of the secondary drops produced by the splash of primary drop falling at an angle of 45° to the plane of the liquid surface and moving above the liquid surface, we used a second Panasonic RX3 analog video camera (not shown in the figure), which recorded the entire space above the point of drop impact on the surface and eventually provide a spatial picture of the interaction.

The drop fall velocity was measured by a time-of-flight method. The system for measuring the drop velocity consisted of an LG-76 continuous-wave laser 8, beam splitters 15, photodetectors 9, a signal shaper and amplifier 13, and an S8-17 double-beam storage oscillograph 14. The plates 15 divide the laser beam, thus forming a changeable base distance required to measure the drop fall velocity. The passage of a falling drop through the laser beam gives two signals, the first of which starts the electrical trigger of the photographic camera and the storage system of the oscillograph. Knowing the distance between the laser beams and determining the time between two signals on the oscillograph, it is possible to determine the drop velocity with a relative error of 5%.

In the experiments, we used a generator of monodisperse drops with four changeable capillaries from stainless steel with polished ends. The size of the generated drops was determined by gravimetric and visual methods. In the gravimetric method, the weight of 100 drops was determined on an analytical balance with subsequent calculation of their diameters. In the visual method, the linear dimensions of falling drops and the geometrical scales of the processes were determined with the use of a reference (a steel bead of 4 mm diameter) placed in the plane of drop fall in the field of shot. The falling-drop size and the other linear dimensions of the process were determined with respect to the reference dimensions from the film carrier or the TV screen. The error of the gravimetric method was 0.5%, the error of the visual method was 5%, and the shooting speed was 24 frames/sec.

The approximate sizes of the initial drops were estimated using the following formula derived from the condition of balance between the gravity and surface tension at the moment of the drop separated from the capillary:

$$D = \left(\frac{\sigma k d}{\rho g}\right)^{1/3}. \tag{1}$$

Here D is the drop diameter, σ is the surface tension of the liquid, d is the capillary diameter, ρ is the density of the liquid, g is the acceleration of gravity, and k a factor that takes into account the narrowing of the neck during drop formation.

The sizes of the capillaries and distilled-water drops ($\rho = 10^3$ kg/m^3 and $\sigma = 72.53 \cdot 10^{-3}$ N/m) are given in Table 1. For $k = (D_{\text{exp}}/D_{\text{calc}})^3$, the error in determining the drop diameter by formula (1) is below 3%.

TABLE 1

d, mm	D, mm			k
	Calculation	Gravimetric method	Visual method	
3.55	5.4	5.03	5.0	0.81
2.20	4.6	4.32	4.3	0.83
1.60	4.1	3.94	4.0	0.86
1.05	3.6	3.66	3.7	1.05

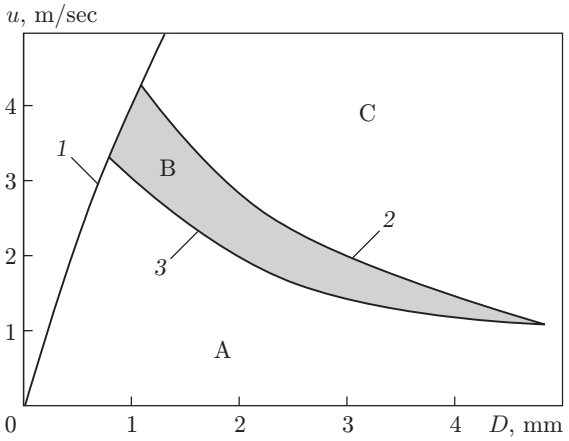

Fig. 2. Boundaries separating the regimes of interaction of a drop with the liquid surface.

Results. Dimensional analysis shows that the problem considered (for the case of a spherical primary drop) is completely characterized by three similarity criteria — the Reynolds (Re), Weber (We), and Froude (Fr) numbers:

$$\mathrm{Re} = \frac{\rho u D}{\mu}, \qquad \mathrm{We} = \frac{\rho u^2 D}{\sigma}, \qquad \mathrm{Fr} = \frac{u^2}{gD}.$$

Here u is the interaction rate (the drop velocity at the moment of impact on the liquid surface), μ is the liquid viscosity, and ρ is the liquid density.

In the present study, distilled water ($\mu = 10^{-3}$ Pa $\cdot$ sec) was used as the model liquid; therefore, the effect of the Reynolds number is insignificant (Re $\approx 10^4$). Three qualitatively different scenarios of the process can be distinguished, depending on the values of the Weber and Froude criteria [6]. In the these coordinates (We and Fr), the boundaries separating these regimes can be represented as the following criterial relations [8], obtained by processing of experimental data [6]:

$$\begin{aligned} &\mathrm{We}_1 = 48.3 \cdot \mathrm{Fr}^{0.247} \qquad \text{for high bound;} \\ &\mathrm{We}_2 = 41.3 \cdot \mathrm{Fr}^{0.179} \qquad \text{for lower boundary.} \end{aligned} \tag{2}$$

The regions with different interaction regimes are illustrated by a plot in the coordinates u and D [see Fig. 2, where curve 1 is the dependence of the maximum (steady-state) velocity of gravitational deposition of a water drop in air on the drop diameter and curves 2 and 3 are the upper and lower boundaries corresponding to relation (2)].

At low interaction rates (region A), the falling drop merges with the liquid without formation of secondary drops. In region B (which is rather narrow), the bubble is entrained in the liquid. We note that this region is characterized by intense entrainment of air bubbles in the liquid at the cavern bottom, leading to increased underwater acoustic noise [6, 8]. In region C, the energy of the cavern being formed is high enough and the process involves formation of secondary drops. The relation $u(D)$ is obtained by solving the equation of gravitational deposition of the drop

$$m \frac{du}{dt} = mg - C_D S \frac{\rho u^2}{2}, \tag{3}$$

TABLE 2

u, m/sec	D, mm								
	0.1	0.2	0.4	1.0	2.0	3.0	4.0	5.0	6.0
Experiment	0.27	0.72	1.62	4.03	4.69	8.06	8.83	9.09	9.18
Calculation	0.24	0.69	1.59	3.88	7.08	8.60	9.93	11.10	12.16

TABLE 3

h, m	u, m/sec	H, mm		$2R$, mm		h_p, mm	
		exp.	calc.	exp.	calc.	exp.	calc.
0.45	2.8	9	13	23	26	27	46
0.70	3.6	13	15	22	32	23	61
0.95	4.1	13	16	26	32	32	70
1.27	4.6	13	17	28	34	32	81
1.73	5.4	13	18	31	36	30	93

where $S = \pi D^2/4$ is the midship-section area of the drop, $m = \pi D^3 \rho/6$ is the weight of the drop, and C_D is the resistance coefficient. The value of C_D was determined from the Klyachko relation [13]

$$C_D = 24/\,\mathrm{Re} + 4/\sqrt[3]{\mathrm{Re}}.$$

Since the greatest ejection of secondary drops occurs at high interaction rates, we studied the characteristics of the process for values $\mathrm{We} > \mathrm{We}_1$. In the experiments, the initial drop diameter was $D = 2.8$–5.0 mm and the fall height was $h = 0.45$–1.73 m. In this case, the interaction rate varied in the range $u = 2.8$–5.4 m/sec, i.e., the parameter values were in region C.

The observation results show that the raindrop diameter varies from 0.2 to 7 mm [14]. Larger drops are deformed and fragmented under the action of aerodynamic forces. Table 2 gives experimental values of the steady-state velocity of water drops in air at atmospheric pressure and temperature 20°C and the velocities calculated from Eq. (3) [14]. A comparison of the rates given in Tables 3 and 4 and the steady-state velocities of drops of the corresponding sizes (see Table 2) shows that in the present experiments, the drops did not reach a steady-state velocity and moved with acceleration.

An analysis of the experimental results indicates that the qualitative picture of the process depends greatly on the interaction rate and, in some cases, can differ considerably from the well-known scenarios [1–9]. Let us consider, in particular, the interaction of a drop of diameter $D = 5$ mm (see Table 3).

The experimental characteristics (cavern depth H, diameter $2R$ measured at the liquid-surface level, and the height of the Rayleigh column h_p) were obtained by averaging over ten identical experiments. At a confidence coefficient of 0.95, the relative error (spread in data) of all linear dimensions of the processes occurring in air and in the water volume does not exceed 12–15% and 5–7%, respectively.

The fall of a drop from a height of 0.45 m on the liquid surface leads to the formation of a small crater and a liquid roller, which in $t \approx 150$ msec, become a Rayleigh column of diameter $d_p \approx 4$ mm and height $h_p \approx 30$ mm. The maximum ratio of the column height to its diameter is $h_p/d_p \approx 7$. During the time of existence of the column ($t \approx 200$ msec), a large spherical drop of diameter $D \approx 6$ mm finally forms at the top of the column, subsequently, separating from the base, it falls after the collapsing column. The further development, i.e., the formation of a new cavern and a new Rayleigh column ceases when this drop falls in the cavern.

The fall of a drop from a height $h = 1.27$ m results in the formation of a spherical cavern of diameter $2R$ = 27–29 mm and depth H = 12–14 mm and a corona with walls standing upright from the crater walls; the diameter of the corona is $d_\mathrm{c} \approx 30$ mm and its height is $h_\mathrm{c} \approx 14$ mm. The top of the corona is formed by 10–15 secondary drops with a diameter $D \approx 0.5$–2 mm, some of which are separated from the corona. The further development of the process leads to the disappearance of the cavern and corona and the formation of a Rayleigh column of diameter d_p = 6–7 mm and height $h_p \approx 30$ mm. The time of formation of the Rayleigh column is $t \approx 80$–100 msec, and the time of its existence is $t \approx 250$ msec. In this case, as is evident from the camera records of the process, the column does not break up. It collapses, leading to the formation of a new cavern and a new roller of smaller

TABLE 4

D, mm	h, m	u, m/sec	H, mm	h_p, mm
2.8	0.45	2.8	7	23
3.7	0.45	2.8	8	24
4.0	0.45	2.8	9	24
4.3	0.45	2.7	9	24
5.0	0.45	2.8	9	27
2.8	0.95	4.0	9	28
3.7	0.95	4.0	9	29
4.0	0.95	4.1	10	31
4.3	0.95	4.0	11	32
5.0	0.95	4.1	13	32

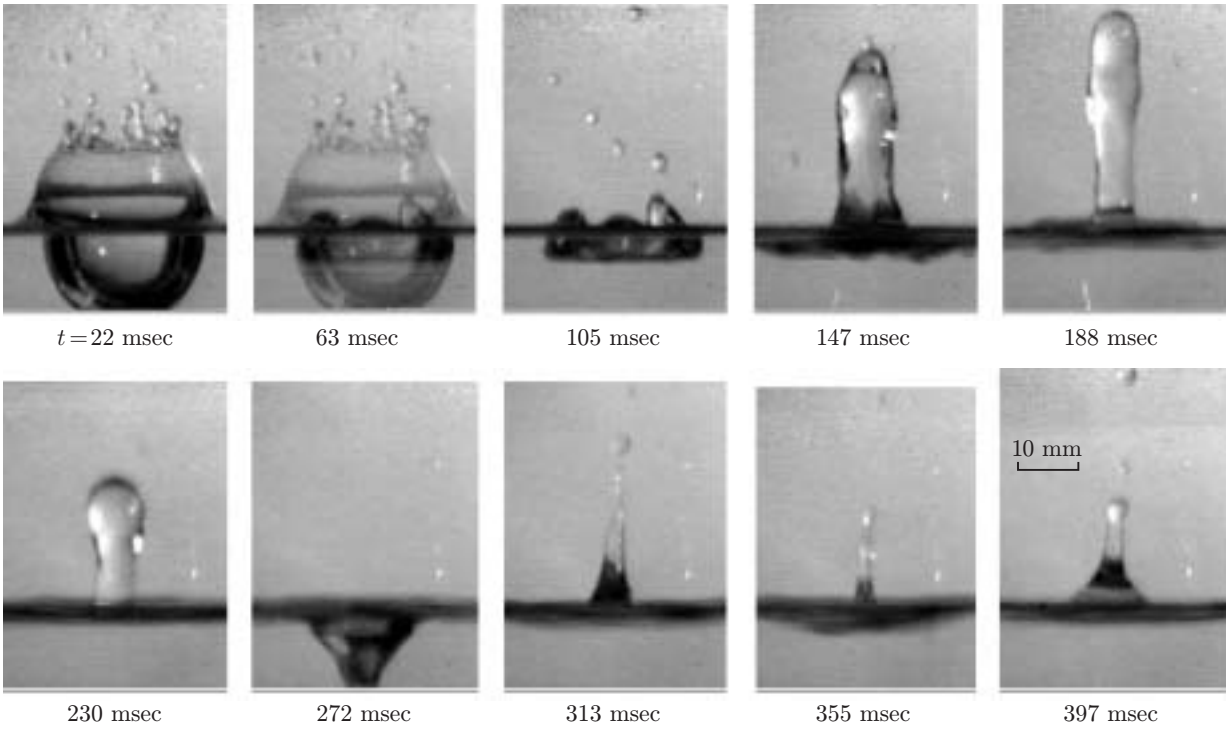

Fig. 3. Camera records of drop impact on the liquid surface ($D = 5$ mm, $h = 1.73$ m, and $u = 5.4$ m/sec).

sizes, whose dynamics results in formation of a secondary Rayleigh column of diameter $d_p = 1.5$–2 mm and height $h_p = 20$–30 mm. This column subsequently disintegrates into three or four drops with diameters of 2–3 mm; i.e., only the secondary Rayleigh column results in formation of secondary drops.

The fall of a drop from a height of 1.73 m (Fig. 3) results (in a time of 80–100 msec) in the formation of a spherical cavern of diameter $2R \approx 30$ mm and depth $H \approx 13$–14 mm and a corona which tends to produce a dome over the cavern of diameter $2R \approx 30$ mm and height $h \approx 14$ mm with subsequent formation of 10–15 secondary drops of 0.5–2 mm diameter. In some experiments, the dome closes to produce a bubble with a dome height H. The dynamics of bubble development and disappearance was not studied in the present work. The further development of the process leads to the picture described above (formation of a cavern and a Rayleigh column and breakup of the latter).

Experimental results for drops of other sizes and various heights of fall are presented in Table 4. We note that an air bubble forms in a certain range of the similarity parameters in the initial stage of the process. Breakup of the bubble results in the formation of fine drops of water aerosol (see, for example, the times 22 and 63 msec in Fig. 3). The total mass of these drops is small but their contribution to the contamination of the neighborhood of

catch basins can be significant because of the processes of aerodynamic transfer and turbulent diffusion. To estimate the degree of dispersion of these drops, it is expedient to use optical methods based on solving inverse problems of aerosol optics (the small-angle scattering indicatrix method and the spectral transparency method) [15].

Analysis of Results. To analyze the results obtained, we estimate the basic characteristics of the process the radius of the cavern R and the height of the Rayleigh column h_p. We assume that the energy of a falling drop is completely expended only in the formation of a hemispherical cavern of radius R in the liquid, which, in turn, completely transfers the energy acquired from the drop to form a Rayleigh column [3, 7].

The total energy of the drop consists of kinetic energy and surface tension energy:

$$E = \pi D^3 \rho u^2/12 + \pi D^2 \sigma. \tag{4}$$

The work of formation of a hemispherical cavern in a liquid consists of the work of formation of its surface and the work done to move the liquid in the gravity field (against the Archimedes forces)

$$A_1 = \pi\sigma R^2 + \pi\rho g R^4/4. \tag{5}$$

Equating relations (4) and (5), we obtain the biquadratic equation for R, whose solution gives the formula for the radius of the cavern:

$$R = \sqrt{\frac{2}{\rho g}} \left\{ \left[\sigma^2 + \rho g D^2 \Big(\sigma + \frac{\rho D u^2}{12} \Big) \right]^{1/2} - \sigma \right\}^{1/2}. \tag{6}$$

The work of formation of the Rayleigh column consists of the work of formation of its surface and the work done to move the liquid under gravity

$$A_2 = \pi d_p h_p \sigma + 0.125 \pi \rho g d_p^2 h_p^2. \tag{7}$$

Equating relations (5) and (7), we obtain the quadratic equation for the product $(d_p h_p)$. Solving this equation and assuming, as follows from the experiments, that $d_p \approx D/2$, we obtain the following formula for the height of the Rayleigh column:

$$h_p = \frac{4}{\rho g D} \left\{ \left[\sigma^2 + \frac{\rho g D^2}{2} \Big(\sigma + \frac{\rho D u^2}{12} \Big) \right]^{1/2} - \sigma \right\}. \tag{8}$$

The values of R and h_p calculated by formulas (6) and (8) for the conditions of the present experiments are given in Table 3. As follows from the measurement data, the geometrical characteristics of the cavern and Rayleigh column vary nonmonotonically as the velocity increases.

As the drop size and the interaction rate increase, the depth of the cavern and the height of the Rayleigh column increase monotonically in the considered range of the parameters (see Table 4). In this case, $d_p = (0.8–1.2)D$. From the results one can see that the calculated values of H, $2R$, and h_p differ considerably from the experimental values since the calculations ignored the energy expenditure in the formation of waves and fine secondary drops produced at the moment of breakup of the corona. In the theoretical consideration, the shape of the cavern was considered hemispherical but in practice it has this shape only at a certain time, after which its shape changes.

Conclusions. The proposed technique can be used in experimental studies of the impact interaction of drops with a liquid surface, a liquid film, and a solid surface.

The results of the present study of drop impact on a liquid surface using the technique showed that in the studied range of the determining parameters, there are several mechanisms by which secondary drops of various degrees of dispersion form:

— Breakup of the corona with the formation of 10–15 drops with a diameter of 0.5 to 2 mm;

— Breakup of the Rayleigh column with the formation of one large drop with a diameter of approximately 6 mm;

— Breakup of the secondary Rayleigh column with the formation of three or four drops with diameters of 2 to 3 mm;

— The height of rise of secondary drops above the liquid surface does not exceed 40–60 mm.

This work was supported by the Russian Foundation for Basic Research (Grant No. 02-01-01246) and the Ministry of Education of the Russian Federation (Grant No. E02-12.3-108).

REFERENCES

1. A. M. Worthington, "The splash of a drop and allied phenomena," *Proc. Roy. Soc. London*, **34**, 217 (1882).
2. L. D. Mahajan, "Liquid drops on the same liquid surface," *Nature*, **126**, No. 3185, 761–767 (1930).
3. O. G. Engel "Crater depth in fluid impacts," *J. Appl. Phys.*, **37**, No. 4, 1798–1808 (1966).
4. P. V. Hobbs and A. J. Kezweeny, "Splashing of a water drop," *Science*, **155**, No. 3766, 1112–1114 (1967).
5. A. D. Solov'ev, "Merging of liquid drops upon impacts," in: *Transactions of the Central Aerological Observatory*, No. 89: *Physics of Clouds and Artificial Effects* [in Russian], Moscow (1969), pp. 3–25.
6. H. C. Pumphrey, L. A. Crum, and L. Bjorno, "Underwater sound produced by individual drop impacts and rainfall," *J. Acoust. Soc. Amer.*, **85**, 1518–1526 (1989).
7. V. V. Mayer, *Cumulative Effect in Simple Experiments* [in Russian], Nauka, Moscow (1989).
8. H. N. Oguz and A. Prosperetti, "Bubble entrainment by the impact of drop on liquid surfaces," *J. Fluid Mech.*, **219**, 143–179 (1990).
9. G. G. Korotkov, "Numerical experiment in problems of an ideal incompressible liquid with free boundaries," Candidate's Dissertation in Phys.-Math. Sci., Kemerovo (2002).
10. M. A. Lavrent'ev and B. V. Shabat, *Problems of Hydrodynamics and Their Mathematical Models* [in Russian], Nauka, Moscow (1977).
11. V. A. Arkhipov, A. P. Berezikov, Yu. A. Biryukov, et al., "Radioactive contamination of ecosystems near open catch basins," in: *Proc. Int. Conf. on the Ecology of Siberia, Far East, and the Arctic Region,"* (Tomsk, September 5-8, 2001), Tomsk, International Research Center for the Physics of the Environment and Ecology, Tomsk Research Center, Siberian Division of the Russian Academy of Sciences (2001), p. 46.
12. V. F. Trofimov, B. B. Baidyusenov, Yu. V. Lim, and A. V. Telgerekov, "Setup for integrated investigation of the interaction of monodisperse drops with a liquid surface," in: *Studies on Ballistics and Related Problems of Mechanics* (collected scientific papers) [in Russian], No. 4, Tomsk State Univ., Tomsk (2001), pp. 25–26.
13. L. S. Klyachko, "Equation of motion for dust particles in dust-receiving devices," *Otopl. Ventil.*, No. 4, 27–29 (1934).
14. P. N. Tverskoi, *Course of Meteorology* (*Atmospheric Physics*) [in Russian], Gidrometeoizdat, Leningrad (1962).
15. V. A. Arkhipov, *Laser Diagnostics for Heterogeneous Flows* [in Russian], Tomsk State Univ., Tomsk (1987).